Behavior of extraordinary rays in uniaxial crystals

Zhongxing Shao and Chen Yi

We have experimentally investigated the behavior of extraordinary rays (E rays) in uniaxial crystals for two cases: that in which optical axes are parallel to the surfaces and that in which they are inclined. The E ray always rotates around the ordinary ray (O ray) in the same direction that the crystal rotates around its surface normal. For the case when the axes are parallel to the surface, we discovered that the E ray rotates up to $\alpha = 2\pi$ as the crystal rotates to $\phi = \pi$. The E ray traces a series of ellipses as the angle of incidence is varied. Snell's law is valid for the E ray only when the optical axes are perpendicular to the plane of incidence. For the case in which the optical axes are incident, the E ray and the crystal rotate at different speeds except for the case of normal incidence. The speed of rotation increases with the incidence angle. The ray traces a curve known as the Pascal worm, which is described by the equation $(x^2 + z^2 - mx)^2 = n^2(x^2 + z^2)$. When the optical axes coincide with the plane of incidence, the space between the rays in the plane is not related to the angle of incidence.

Introduction

Double refraction is an important and basic phenomenon in crystal optics. The fact that the ordinary (O) ray of double refraction obeys Snell's law is well known. However, the behavior of the extraordinary (E) ray, to the best of our knowledge, is not thoroughly understood.[1–4] In Ref. 1 it was deduced that each double refraction obeys the same law of refraction. Determination of the direction of propagation of the E ray is more complicated because the index of the ray depends on the refractive angle. However, traces of the E ray in uniaxial crystals have been calculated by some authors.[5–7]

In recent years there have been numerous applications of double refraction in the area of laser and nonlinear optics. For example, birefringent filters acting as effective dispersion elements have been applied widely in some tunable lasers. Frequency doublers are the key to expanding the laser wavelength, and other crystal devices are important for the generation of nonlinear optical effects. To achieve the best design of these optical elements, one must know the behavior of the E ray.

Here we report on an experimental investigation of the behavior of the E ray, including rotating direction and speed, traces, and some features about the traces. We used two pieces of calcite: one with the optical axis parallel to the surface (APS) and the other with the axis incident to the surface (AIS). Interesting results were observed and are discussed.

Experiments and Results

The experimental setup is simple. The APS of the calcite cuboid and the AIS of the calcite [which has natural cleavage; the axis makes an angle $\gamma = 45.93°$ (Ref. 7) with the three planes intersecting at the vertex A or A′ (see Fig. 1)] are illuminated by the beam of a He–Ne (633-nm) laser through a telescope system. The crystal thicknesses are 8.5 and 21.2 mm, respectively. They are mounted so that they rotate both horizontally and vertically. In fact the crystals were not processed precisely, and there is a wedge (of $\sim 3°$) formed by the surfaces of each one.

In these experiments one must be sure that the observer is not confused by the refraction at the rear surface of the crystal. The rear surface is wedged with respect to the front surface, although possibly by only a small amount. For this reason we observed the beam spots on the rear surface directly.

Taking incidence angles of $\theta = 0, \pi/6, \pi/4, \pi/3, 5\pi/12$ and twisting the APS crystal from the angle $\phi = 0$ (the optical axes are in the incident plane) to π in steps of $\pi/16$ and from $\phi = 0$ to 2π in steps of $\pi/8$ for the AIS crystal, we took pictures of the E and the O rays at the rear surface with a camera aimed at the spots. The spaces between the spots of the two rays in the negatives were measured with a reading microscope. The spaces are fractions of a millimeter, and the measuring error is ± 0.01 mm, so that the relative

Z. Shao is with the Changchun Institute of Optics and Fine Mechanics, P.O. Box 1024, Changchun 130022, China. C. Yi is with the Jilin Institute of Lasers, Changchun, China.

Received 15 September 1992; revised manuscript received 1 April 1993.

0003-6935/94/071209-04$06.00/0.

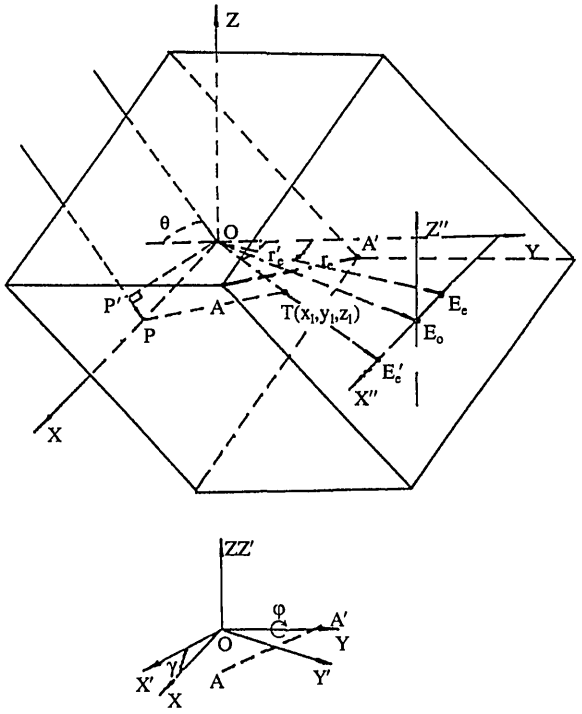

Fig. 1. Diagram showing double refraction in a uniaxial crystal. The figure at the bottom shows the rotation of the $X'Y'Z'$ system with respect to the XYZ system.

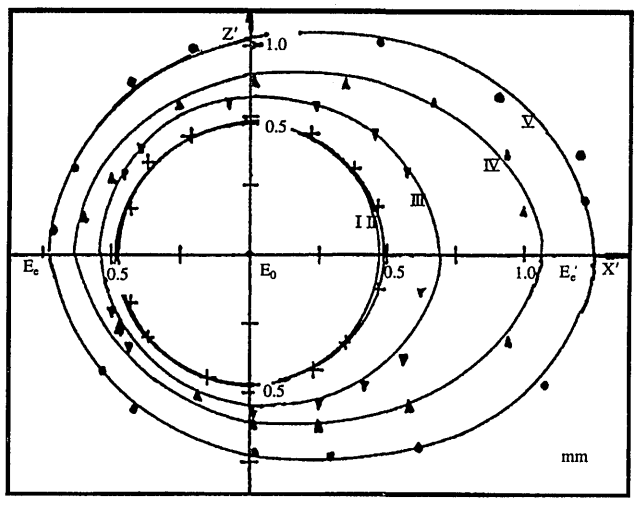

Fig. 2. Traces of the E ray on the rear surface of the calcite APS at a different incidence. The O ray acts as the origin of the coordinates, the X'' axis is parallel to the X axis. Curves I–V are the traces for $\theta = 0, 5\pi/12, \pi/3, \pi/4, \pi/6$, respectively. The symbols on the curves denote the rotation of the crystal in steps of $\phi = \pi/16$: ●, curve V; ▲, curve IV; ▼, curve III; +, curve II.

precision is better than 10%. The experimental error is estimated to be less than 10%.

For the APS calcite, the E ray always rotates to the angle $\alpha = 2\pi$ around the O ray, no matter what the angle of incidence is, whereas the crystal is rotated to $\phi = \pi$ around its normal. This result agrees with the theoretical calculation in Ref. 7. The ray rotates in the same direction as the crystal but not at the same speed. At large angles of incidence, α equals approximately $8\phi/5$ within the first quadrant in the coordinate system where the origin is at the O ray, and the positive X axis coincides with the optical axis in the plane of incidence; $\alpha = 2\phi$ in the second and the fourth quadrants, and $\alpha = 8\phi/3$ in the third as in the first quadrant. The traces of the ray are a series of ellipses where the axes coincide with the coordinate axes. The centers of the ellipses are at the X axis but not at the O ray (see Fig. 2), which makes us believe that these ellipses are not geometrically formed by the oblique arrangement of the crystal. Also, we believe that the circular trace for the case of normal incidence is due to the unparallel surfaces. The larger the angle of incidence becomes, the flatter the ellipses become. The axes of the ellipses, a and b, are listed in Table 1.

In the AIS case, if the crystal is rotated to $\phi = 2\pi$, the E ray rotates to $\alpha = 2\pi$ in contrast to the APS case. In Fig. 3 we find that the rotating speed of the ray is not in step with the crystal. At incidences larger than $\pi/4$, since the optical axis is close to making an acute angle γ to the X axis in the plane of incidence, the ray stays close to the plane even though the axis might be rotated far from the plane. On the other hand, in the vicinity of the obtuse angle $\pi-\gamma$, the ray runs much faster than the axis. At a small incidence, less than $\pi/6$, the ray generally keeps in step with the axis and is exactly in step with the axis only at normal incidence. For each $\alpha = \pi/2$, the average ϕ and α/ϕ are listed in Table 2.

The E-ray traces in Fig. 3 (the solid curves) are perfectly consistent with the Pascal worm (the dashed curves) described by the equation $(x^2 + z^2 - mx)^2 = n^2(x^2 + z^2)$, where the constants m and n for each worm are listed in Table 2. The traces look as if they are slightly asymmetrical to the coordinate axes, which might be attributed to the crystal surfaces not being exactly parallel. It is interesting to note that all the distances between the coordinates of the traces on the X and Y axes are the same as 4.55 mm. The coordinates of the traces on the Y axis are symmetrical to the origin, however; on the X axis they do not increase the incidence. It looks as if the circular trace at normal incidence is thrown in the positive X-axis direction, whereas the spaces on the coordinate axes remain fixed.

Geometry

The fixed coordinate system XYZ is set so that the behavior of the E rays can be observed, and the

Table 1. Axes *a* and *b* of the Ellipses in Fig. 2 for Different Angles of Incidence

θ	*a* (mm)	*b* (mm)
0	0.45	0.45
π/6	0.46	0.44
π/4	0.60	0.56
π/3	0.81	0.61
5π/12	0.98	0.74

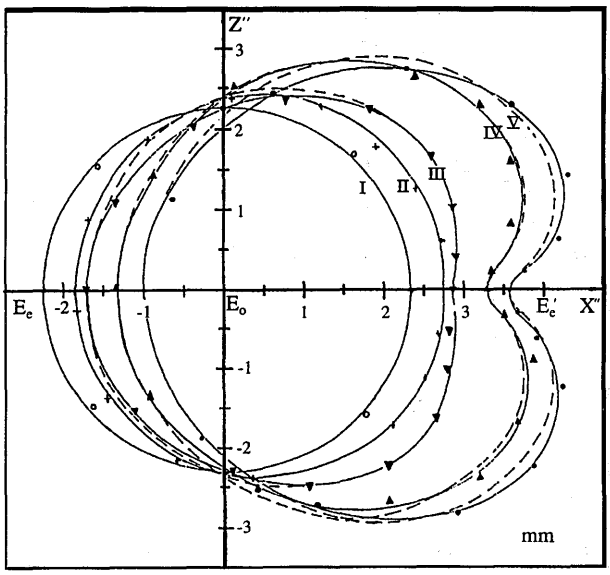

Fig. 3. Traces of E rays of the calcite AIS (natural cleavage). The solid curves are the experimental results, the dashed curves are the Pascal worm calculated by $(x^2 + z^2 - mx)^2 = n^2(x^2 + z^2)$. The symbols denote the rotation of the crystal in steps of $\phi = \pi/8$. The other factors are the same as in Fig. 2. ●, curve V; ▲, curve IV; ▲, curve III; +, curve II; ○, curve I.

primed system $X'Y'Z'$ is fixed in the crystal with the optical axis parallel to the X' axis in the $X'Y'$ plane and rotates with it. When the primed system $X'Y'Z'$ rotates first through γ around the Z' axis and then through ϕ around the Y' axis (see the diagram at the bottom of Fig. 1), the ray satisfies the ellipsoidal equation in terms of the system XYZ:

$$(A\cos^2\phi + n_e^2\sin^2\phi)x^2 + By^2 + (A\sin^2\phi + n_e^2\cos^2\phi)z^2 + 2C\cos\phi xy + 2C\sin\phi yz + 2D\sin\phi\cos\phi zx = 1, \quad (1)$$

where

$$A = n_o^2\cos^2\gamma + n_e^2\sin^2\gamma,$$
$$B = n_o^2\sin^2\gamma + n_e^2\cos^2\gamma,$$
$$C = (n_e^2 - n_o^2)\sin\gamma\cos\gamma,$$
$$D = (n_o^2 - n_e^2)\cos^2\gamma.$$

Here n_o, n_e are the principal indices of refraction of the O and the E rays, respectively.

Now we discuss some issues concerning the traces of the E ray in the AIS calcite. First we consider the case of $\phi = 0$, or the optical axis in the XY plane. The experiments tell us that the ray is in the plane, namely, $z = 0$. Then the expression about the plane tangent to the E-ray wave surface through point $T(x_1, y_1, z_1)$ (Fig. 1), which we obtain by substituting the coordinates of T into Eq. (1), is

$$Ax_1x + By_1y + C(y_1x + x_1y) = 1. \quad (2)$$

On the other hand, because $PP' = ct = x\sin\theta$ (c is the speed of light, t is time), the coordinates at point P are $(1/\sin\theta, 0, 0)$ when $t = 1/c$. Substituting the coordinates of P into Eq. (2), we have

$$Ax_1 + Cy_1 - \sin\theta = 0$$

or

$$y_1 = (\sin\theta - Ax_1)/C. \quad (3)$$

Because point T is in the tangent plane, Eq. (2) with respect to T can be rewritten as

$$Ax_1 + By_1 + 2Cx_1y_1 = 1. \quad (4)$$

Considering Eqs. (3) and (4), we have

$$x_1 = (\sin\theta \pm CK)/A,$$
$$y_1 = k,$$

(+ is the axis at the acute angle to the positive X axis, − is the axis at the obtuse angle), where

$$k = [(A - \sin^2\theta)/(AB - C^2)^{1/2}].$$

In the light of x_1 and y_1 the refractive angles between the ray on both sides of the O ray and the Y axis (the normal of the crystal) are

$$r_e' = \arctan[(\sin\theta + CK)/(AK)], \quad (5)$$

$$r_e = \arctan[(\sin\theta - CK)/(AK)], \quad (6)$$

respectively, and the spaces Δ between the coordinates, E_e and E_e', of the traces on the X'' axis that are parallel to the X axis (see Fig. 3) are

$$\Delta = d[\tan(r_e') - \tan(r_e)] = 2dC/A. \quad (7)$$

Table 2. Data in the Experiments and Comparison between the Data and Theoretical Calculation[a]

	Quad. I, IV		Quad. II, III				r_e (deg)		r_e' (deg)	
θ	ϕ	α/ϕ	ϕ	α/ϕ	m (mm)	n (mm)	Cal.	Exp.	Cal.	Exp.
0	$\pi/2$	1	$\pi/2$	1	0	2.28	6.19	6.13	6.19	6.13
$\pi/6$	$5\pi/8$	4/5	$3\pi/8$	4/3	4.10	0.45	12.72	13.02	23.87	24.04
$\pi/4$	$3\pi/4$	2/3	$\pi/4$	2	3.40	1.11	21.46	21.33	31.38	31.13
$\pi/3$	$>3\pi/4$	$<2/3$	$<\pi/4$	>2	2.41	2.25	28.77	28.70	37.45	37.53
$5\pi/12$	$>3\pi/4$	$<2/3$	$<\pi/4$	>2	2.28	2.28	33.71	33.90	41.48	41.52

[a] θ, incidence; ϕ, rotation of the crystal; α, rotation of the E-ray around the O ray; m and n, constants in the Pascal equation; r_e and r_e', refractive angles between the E-ray incident upon the X'' axis (see Fig. 3) and the normal.

So far, we have been able to understand, in the light of Eq. (7), why the spaces are constant as the angle of incidence varies. It turns out that Δ is not related to the angle of incidence but only to the angle γ. So we infer that the same γ would cause the same Δ, no matter what the angle of incidence is.

If $\theta = 0$ (normal incidence), in addition, in the light of Eqs. (5) and (6) the refractive angle

$$r_e' = \arctan(C/A) = -r_e.$$

In our situation $r_e' = 6.186°$ by calculation and 6.125° by experiment. This is a good agreement. In Table 2 r_e' and r_e are listed for different angles of incidence.

To discuss the traces of the E ray in the APS crystal, we simply make $\gamma = 0$ in Eq. (1). For $\phi = 0$, we have

$$n_o^2 x_1 x + n_e^2 y_1 y = 1. \tag{8}$$

Applying the coordinates of point P to Eq. (8), we obtain

$$x_1 = \sin\theta/n_o^2,$$
$$y_1 = [1 - (\sin\theta/n_o)^2]^{1/2}/n_e.$$

Similarly, when $\phi = \pi/2$,

$$x_1 = \sin\theta/n_e^2,$$
$$y_1 = [1 - (\sin\theta/n_e)^2]^{1/2}/n_e.$$

Imitating the form of Snell's law, we have for $\phi = 0$

$$\sin\theta/\sin(r_e) = n_e(\theta) \tag{9}$$

with

$$n_e(\theta) = [n_o^4 + (n_e^2 - n_o^2)\sin^2\theta]^{1/2}/n_e. \tag{10}$$

Apparently Eq. (9) is inconsistent with Snell's law because $n_e(\theta)$ depends on the incidence. However, for $\phi = \pi/2$,

$$\sin\theta/\sin(r_e') = n_e.$$

Equation (10) is just the familiar Snell's law. So we can deduce that for Snell's law to be valid for the E ray the optical axes must be perpendicular to the plane of incidence.

Conclusions

We have studied the behavior of the E ray in a uniaxial crystal (calcite). The ray always rotates around the O ray as the crystal is rotated around its normal. The ray does not rotate in step with the optical axes except at normal incidence. For the APS crystal (1) the ray always rotates to the angle $\alpha = 2\pi$ as the crystal is rotated to the angle $\phi = \pi$, (2) the traces of the ray are a series of ellipses, (3) Snell's law is valid for the ray only in the condition in which the optical axes are perpendicular to the plane of incidence. For the AIS case: (1) At the larger angles of incidence, the ray stays close to the plane, although the axis may move far away from the plane. As the axis rotates 180° to the plane, the ray moves faster than the axis. Conversely, at small incidence, the ray rotates approximately in step with the axis and exactly with the axis only at normal incidence. (2) The traces of the ray are perfectly consistent with the Pascal worm described by the equation $(x^2 + z^2 - mx)^2 = n^2(x^2 + z^2)$. (3) When the axes are in the incident plane, the spaces between the E and the O rays in the plane do not change while the incidence is varied.

The authors are grateful to Fengming Xu of the Changchun Institute of Optics and Fine Mechanics for aid. Qingkui Pei and Peifeng Zhang of the Changchun Photon Company for supplying the crystals; J. Bollinger and J. C. Bergquist of the Boulder Laboratory, National Institute of Standards and Technology, for meaningful discussions; J. Gary Eden and his graduate student, Hao C. Tran, the University of Illinois at Urbana–Champaign, for help; and Guangxu Chen and Carolyn Such for proofreading the English.

References

1. M. Born and E. Wolf, *Principles of Optics* (Pergamon, London, 1975), Chap. 14, pp. 676, 685.
2. F. A. Jenkins and H. E. White, *Fundamentals of Optics* (McGraw-Hill, New York, 1976), Chap. 24.9, pp. 508–509.
3. W. H. A. Fincham and M. H. Freeman, *Optics* (Butterworth, London, 1980), pp. 340–341.
4. M. V. Klein and T. E. Furtak, *Optics* (Wiley, New York, 1986), Chap. 9, p. 601.
5. Q. T. Liang, "Simple ray tracing formulas for uniaxial optical crystals," Appl. Opt. **29,** 1008–1010 (1990).
6. M. C. Simon and R. M. Echarry, "Ray tracing formulas for monoaxial optical components: vectorial formulation," Appl. Opt. **25,** 1935–1939 (1986).
7. Z. X. Zhang, Acta Phys. Sin. (in Chinese) **29,** 1483–1487 (1980).